LLRF CONTROLS INCLUDING GAP TRANSIENTS AT KEKB AND PLANS FOR superKEKB

T. Kobayashi† and K. Akai, KEK, Tsukuba, Japan

Abstract

Features of LLRF control systems in KEKB and SuperKEKB will be reviewed, and the evaluation of the bunch gap transient effect on beam phase will be presented for SuperKEKB. The RF systems of KEKB are being reinforced to handle triple as large beam power for upgrade to SuperKEKB. Furthermore, a new LLRF control system, which is based on a recent digital control technique, has been developed. They were worked successfully in the Phase-1 commissioning.

Bunch phase shift along the bunch train due to a bunch gap transient is a concern in a high intensity circular collider. In KEKB operation, a rapid phase change was observed at the leading part of the train in the bunch phase measurement, which was not predicted. Our new simulation study of the bunch gap transient effect on beam phase clarified that the rapid phase change is caused by a transient loading in the three-cavity system of ARES. The new simulation for SupeKEKB shows that the phase change due the bunch gap will be significantly large at the design beam current operation. The main issue is the difference in beam phase change between the two rings for the asymmetry colliding. The measures for mitigation of the relative beam phase difference between the two rings will be also suggested.

INTRODUCTION

KEKB is an asymmetric energy collider consisting of an 8 GeV electron ring (high-energy ring, HER) and a 3.5 GeV positron ring (low-energy ring, LER), which was operated from 1998 to 2010 [1]. It obtained the world record in luminosity of 2.11×10^{34} cm^{-2}s^{-1}. To increase the luminosity, a high-current beam is needed in both rings, which is accomplished by filling bunches into a number of buckets. One serious concern for high-current storage rings is the coupled-bunch instability caused by the accelerating mode of the cavities. This issue arises from the large detuning of the resonant frequency of the cavities that is needed to compensate for the reactive component of the beam loading [2]. Two types of cavities that mitigate this problem are used in KEKB [3, 4]: one is the ARES normal conducting three-cavity system [5, 6] and the other is the superconducting cavity (SCC) [7, 8]. The detuning frequency of these cavities is reduced owing to the high stored energy in these cavities.

The ARES is a unique cavity, which is specialized for KEKB. It consists of a three-cavity system operated in the $\pi/2$ mode: the accelerating (A-) cavity is coupled to a storage (S-) cavity via a coupling (C-) cavity as shown in Fig. 1 [9]. The A-cavity is structured to damp higher-order modes (HOM). The C-cavity is equipped with a damper to damp parasitic 0 and π-modes. The $\pi/2$ mode has a high Q-value even with a C-cavity with a very low Q-value of about 100. In LER, where a higher beam current is stored than in HER, only the ARES cavities were used. For details regarding the RF systems of KEKB, see Refs. [3, 4]. The RF issues to be considered for the heavy-beam current storage are summarized in Ref. [10].

KEKB is being upgraded to SuperKEKB, which is aiming at a 40 times higher luminosity than KEKB [11, 12]. The RF related machine parameters are shown in Table 1. The RF systems are being reinforced to handle twice as large stored beam currents in both rings and much higher beam power (compared to KEKB) [13]. ARES and SCC will be reused with the reinforcements. The RF power source systems, including klystrons, waveguides, and cooling systems, also need to be reinforced to increase the driving RF power to provide larger beam power. Furthermore, a new low-level RF (LLRF) control system, which is based on a recent digital control technique using field-programmable gate arrays (FPGAs), has been developed to realize higher accuracy and greater flexibility [14]. For nine RF stations, among a total of thirty, the LLRF control system used in KEKB has been replaced with new ones.

The first beam commissioning of SuperKEKB (Phase-1) was accomplished in 2016. The RF systems and the new LLRF control systems were soundly worked. The desired beam current of 1A for Phase-1 was successfully achieved and the vacuum scrubbing was sufficiently progressed.

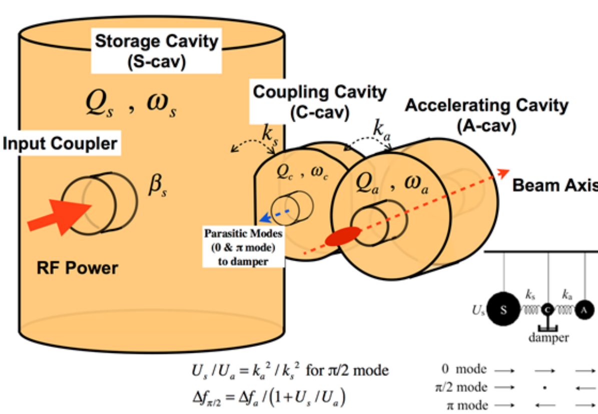

Figure 1: Illustration of the ARES cavity structure.

RF SYSTEM ARRANGEMENT

RF related parameters of SuperKEKB are shown in Table 1 in contradistinction with those of KEKB. The RF system layout of KEKB is shown in Fig. 2. The planed arrangement for SuperKEKB at the design beam current is also shown in the figure (lower side). We have about

ISBN 978-3-95450-187-8

thirty stations of the RF power source (klystron and the LLRF control). SCC's are used in HER. Eight modules of SCC are installed at Nikko section. For the other section, ARES cavity units are used. In LER, all cavities are the ARES type. In the KEKB operation, one klystron has driven two ARES units. On the other, in SuperKEKB, one klystron should drive only one ARES unit (so called "one-to-one configuration" is necessary), because the beam power per ARES will be three times higher than that of KEKB (see Table 1). The cavity input power will be about 750 kW (cavity wall loss + beam power) in SuperKEKB, while the maximum klystron output power is about 1MW. Accordingly additional klystrons are needed for the upgrade. The input coupler of ARES has been already reinforced for the increased input power.

For Phase 1 as a first step, six ARES units of OHO-D5 section were relocated from HER to LER, and the configuration of them was changed to the one-to-one configuration. Additionally the configuration of D7-C, D7-D, D8-C and D8-D stations was also changed to the one-to-one configuration for Phase-1.

Table 1: RF related parameters of KEK and SuperKEKB

Parameter	unit	KEKB (achieved)				SuperKEKB (design)			
Ring		HER			LER	HER		LER	
Energy	GeV	8.0			3.5	7.0		4.0	
Beam Current	A	1.4			2	2.6		3.6	
Number of Bunches		1585			1585	2500		2500	
Bunch Length	mm	6-7			6-7	5		6	
Total Beam Power	MW	~5.0			~3.5	8.0		8.3	
Total RF Voltage	MV	15.0			8.0	15.8		9.4	
		ARES		SCC	ARES	ARES	SCC	ARES	
Number of Cavities		10	2	8	20	10	8	8	14
Klystron : Cavity		1:2	1:1	1:1	1:2	1:1	1:1	1:2	1:1
RF Voltage (Max.)	MV/cav.	0.5		1.5	0.5	0.5	1.5	0.5	
Beam Power (Max.)	kW/cav.	200	550	400	200	600	400	200	600

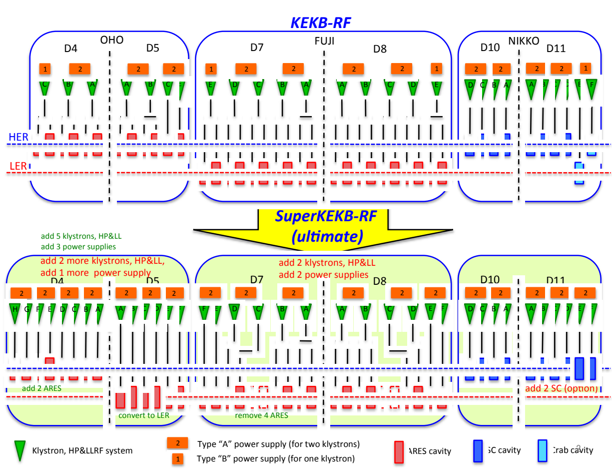

Figure 2: RF system arrangement of KEKB and plan for SuperKEKB ultimate stage.

LLRF CONTROL SYSTEM

Accuracy and flexibility in accelerating field control are very essential for storage of high-current and high-quality beam without instability. Therefore, new low level RF (LLRF) control system, which is based on recent digital architecture, was developed for the SuperKEKB. Figure 3 shows a picture of a mass-production model of the new LLRF system for the SuperKEKB. A block diagram of an ARES cavity driving system is shown Fig. 4. The principal functions of this system are performed by five FPGA boards which work on MicroTCA platform as advanced mezzanine cards [15]: Vc-FB controller (FBCNT), cavity-tuner controller (TNRCNT), inter-lock handler (INTLCNT), RF-level detector for the interlock and arc-discharge photo-signal detector. As shown in Fig. 4, the new LLRF control system handles I/Q components of controlling signals in the FPGAs. For slow interlocks (e.g. vacuum, cooling water) and sequence control, a PLC is utilized. EPICS-IOC on Linux -OS is embedded in each of the FPGA boards and the PLC [16].

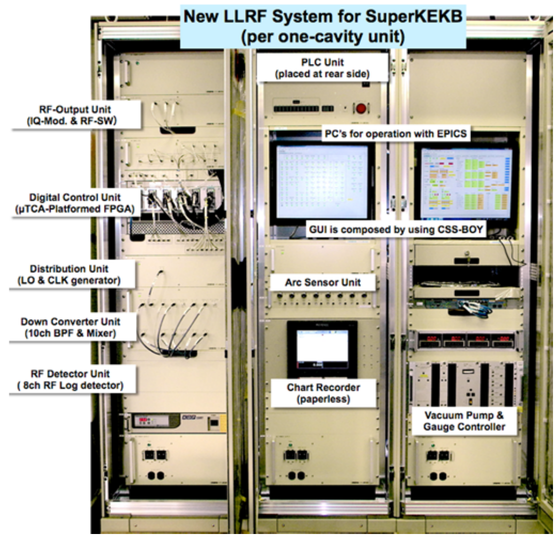

Figure 3: LLRF control system for SuperKEKB.

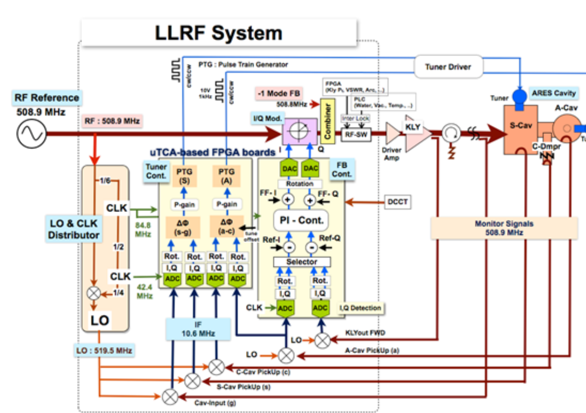

Figure 4: Block diagram for ARES cavity control.

At 9 stations of Oho D4&D5 (6@D5 + 3@D4) , the LLRF control systems were replaced with new digital control systems for Phase-1 as shown Fig. 5 and Fig. 6.

All of new systems successfully worked well without problem. Some software bugs found during the operation were fixed. The DR-LLRF control system has already installed in DR control room. It is almost the same as MR one, except 3-cavity vector-sum control is needed. In the present stage, the number of cavities is two.

On the other hands, the other stations were still operated with existing (old analogue) LLRF control systems, which had been used in the KEKB operation. These systems are composed of combination of NIM standard analogue modules as shown in Fig. 7. They are controlled remotely via CAMAC system. All systems also soundly worked as well as operated in the KEKB operation, although many old defective modules were replaced with spares in the maintenance works.

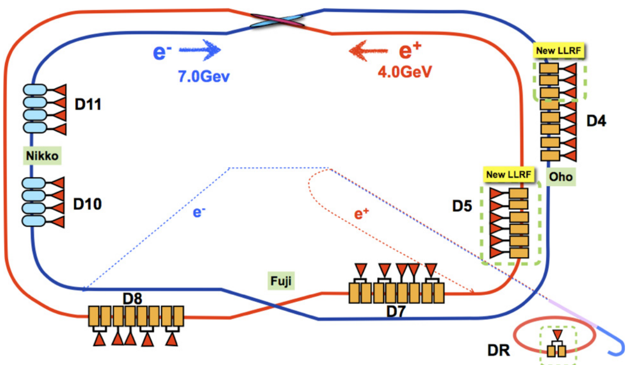

Figure 5: RF system layout for the Phase-1. Nine LLRF stations were replaced with the new ones. DR-LLRF control system was also newly installed.

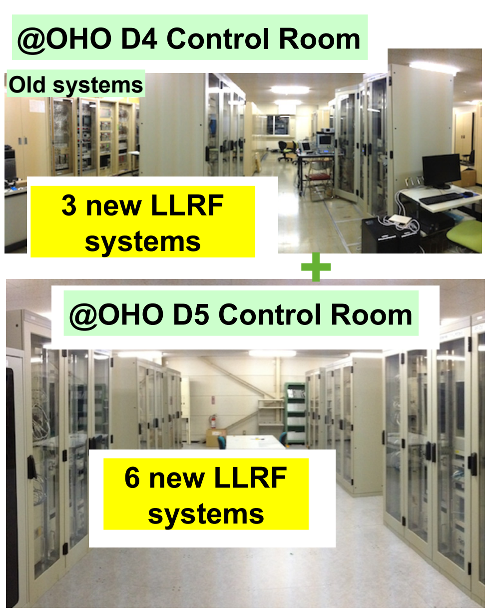

Figure 6: Installation appearance of the new LLRF control systems in the RF control rooms at D4 (upper) and D5 (lower) section.

Figure 7: Old LLRF control system, which was used in KEKB operation, continues in use for SuperKEKB.

RF reference distribution system was also upgrade for SuperKEKB [17]. RF reference signal is optically distributed into 8 sections by means of "Star" topology configuration from the central control room (CCR). "Phase Stabilized Optical Fiber", which has quite small thermal coefficient (< 1ppm/°C), is adapted. For the thermal phase drift compensation, optical delay line is controlled digitally at CCR for all transfer lines as shown in Fig 8. The short term stability (time jitter) is about 0.1 ps (rms), and the long term stability (pk-pk) is ±0.1° = ±0.55 ps at 508.9MHz (expected by the optical delay control).

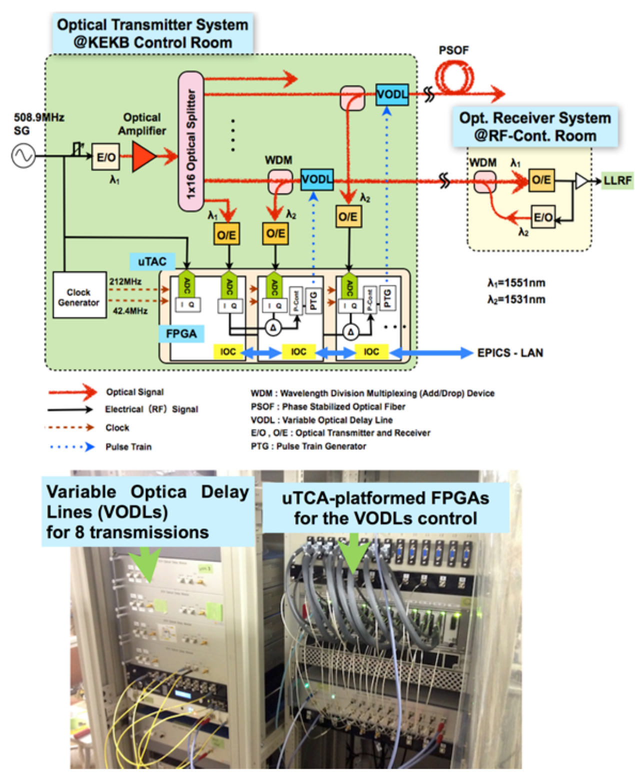

Figure 8: New RF reference signal distribution system for SuperKEKB. Block diagram of the reference distribution (upper side) and the photo of VODL control system (lower side) are shown.

The Phase-1 commissioning result is shown in Fig. 9. History of the stored beam current with beam dose (upper side) and the total acceleration voltage called total-Vc (lower side) of the both ring during Phase-1 is plotted in the figure. RF systems worked well without serious trouble. Target beam current of ~1A for Phase-1 was successfully achieved in both ring and vacuum scrubbing has been sufficiently progressed.

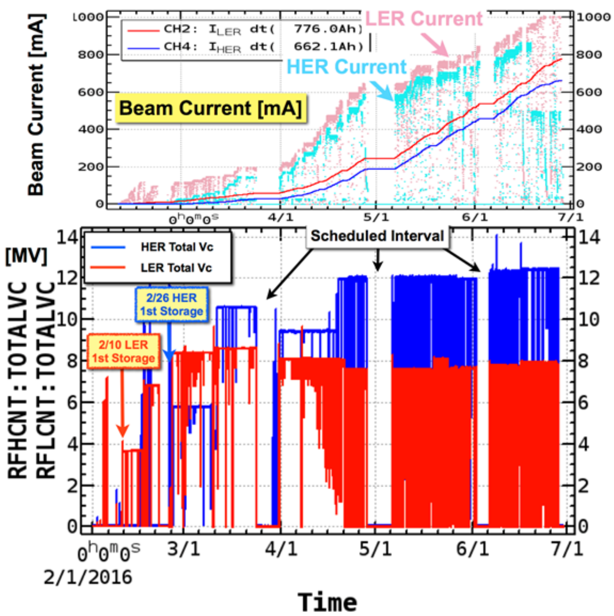

Figure 9: History of the stored beam current, the beam dose (upper side), and the total acceleration voltage called Total-Vc (lower side) for the both ring.

COUPLER BUNCH INSTABILITY DUE TO ACCELATING MODE

In HER, over the 400-mA beam current, the μ=-1 mode instability due to the detuned cavities (parked with some reasons) was excited. It could not be suppressed by the tuner adjustment. Consequently, the μ=-1 mode damper system, which had been used in KEKB operation as shown in Fig. 10, was applied to the D4 station. It worked well to suppress the μ=-1 mode successfully and the beam current could be increased.

Figure 11 shows estimation of the growth rates of the couple bunch instability due to the accelerating mode plotted as function of the stored beam current for SuperKEKB LER (left side) and HER (right side) [18]. The threshold current of the μ=-1 is about 1.8 A for LER and 1.2 A for HER. In Phase-1, at an earlier stage than expected, the μ=-1 mode damper became needed due to the detuned cavities. At the design beam current of SuperKEKB, the growth rate of the μ=-2 mode instability will be close to the radiation damping rate. Therefore, the μ=-2 mode damper system is additionally necessary for Phase-2. New damper system with new digital filters is now under development for Phase-2 [18]. It will be available for μ=-2-1, -2 and -3 modes in parallel as shown in Fig. 12. Respective feedback phase for each mode can be adjusted independently in the digital filter.

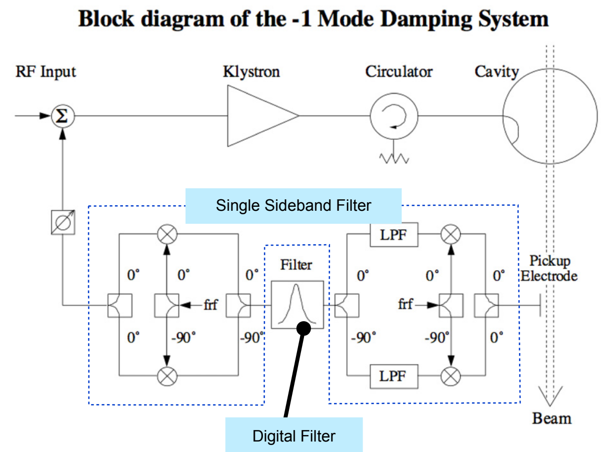

Figure 10: Block diagram of the μ=-1 mode damping system, which had been used in KEKB operation. The μ=-1 mode digital feedback selectively reduces impedance at the driving frequency.

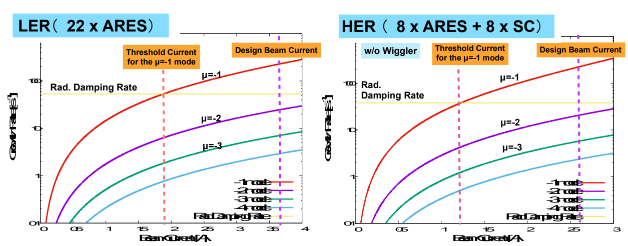

Figure 11: Estimation of the growth rate of the couple bunch instability due to the accelerating mode for SuperKEKB.

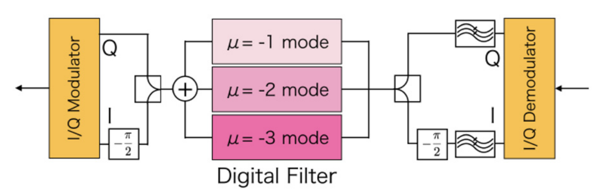

Figure 12: Design concept of the new digital filter with single sideband filter for the couple bunch instability damping system. The digital filter is available for the μ=-1, -2 and -3 modes in parallel.

BUNCH GAP TRANSIENT EFFECT ON BEAM PHASE

In generally, for a high-current multi-bunch storage ring, a bunch train has a gap of empty buckets in order to allow for the rise time of a beam abort kicker. The empty gap is also effective in clearing ions in electron storage rings. However, the gap modulates the amplitude and phase of the accelerating cavity field. Consequently, the

ISBN 978-3-95450-187-8

longitudinal synchronous position is shifted bunch-by-bunch along the train, which shifts the collision point of each bunch in a collider.

Figure 13 shows the beam phase measured along the bunch train in KEKB operation. The abscissa axis indicates the bucket ID. The measured phase shift along the train agreed well with a simulation (solid line) and a simple analytical form given by [19] in most part of the train. However, a rapid phase change was observed at the leading part of the train, which was not predicted by the simulation or by the analytical form. In order to understand the cause of this observation, we have developed an advanced simulation, which treats the transient loading in each of the three cavities of ARES [20], instead of the equivalent single cavity used in the previous simulation. The new simulation result shown Fig. 13 as dashed line reproduces well the observed phase modulation. Accordingly it clarifies that the rapid phase change at the leading part of the train is caused by a transient loading in the three-cavity system of ARES: the rapid phase change is attributed to the parasitic (0&pi) mode of ARES.

Figure 14 shows RF phase modulation of the accelerating cavity of ARES. It was measured by the new digital LLRF control system in the Phase-1 commissioning. The abscissa axis is time in microseconds. The time interval of 10 microseconds is the revolution period. Similarly, the rapid phase change is observed at the leading part of the train. The simulation result (dashed red line) agrees well with the measurement. In the simulation, function of feedback control for cavity voltage regulation by LLRF control system is also included. However, at the leading part of the train, the behaviour of the phase ringing after the raid phase rising disagrees with the simulation. It is considered that the sampling rate of the LLRF system, which is about 10MHz, might not be enough to catch this rapid change of the phase ringing. On another front, the behaviour of this phase ringing at the leading of the bunch train depends strongly on Q-value of the coupling cavity of ARES. The ARES cavity parameters used for the simulation are shown in Table 2. There is possibility that the practical Q-value of the C-cavity in this measurement is lower than 100.

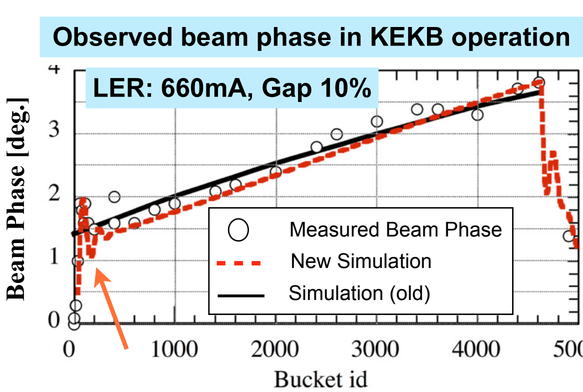

Figure 13: Observed beam phase along the bunch train in the KEKB operation and simulation results.

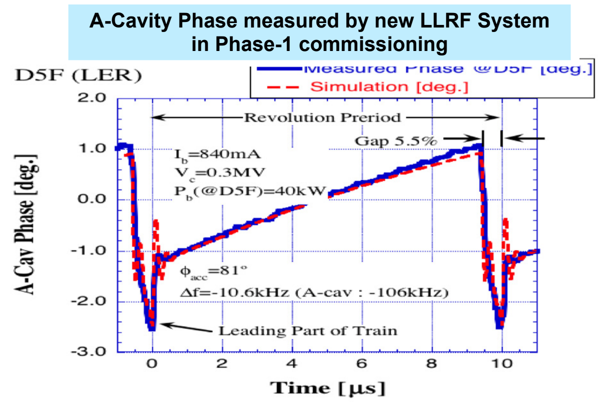

Figure 14: RF phase modulation in the accelerating cavity of ARES, which measured by new LLRF control system in Phase-1 commissioning, and the new simulation result are plotted during the revolution period.

Table 2: ARES cavity parameters used for the simulation

Q-value of A-cavity (Q_a)	26000
Q-value of C-cavity (Q_c)	100
Q-value of S-cavity (Q_s)	180000
Coupling between A and C cavity (k_a)	5%
Coupling between S and C cavity (k_s)	1.6%

ESTIMATION OF BUNCH GAP TRANSIET EFFECT FOR superKEKB

The phase modulation caused by the bunch gap transient was estimated for SuperKEKB by using the new simulation. The operation parameters used for the simulation are shown in Table 3. The length of the bunch gap will be reduced to 2% of the ring in SuperKEKB by improving the rise time of the abort kicker.

Figure 15 shows the simulation results of the phase modulation caused by the bunch gap transient in LER (left side) and HER (right side). The revolution frequency is set to 100 kHz instead of 99.4 kHz to simplify the abscissa axis of time. In the figure, the periodic interval of time 0 to 10 μs corresponds to one revolution, including the 2% empty gap. The time 0 corresponds to the head bunch of the train, and the empty gap is located from 9.8 to 10 μs. For the HER simulation, the vector sum of ARES and SCC was calculated. On the other hand, LER is operated with only ARES type cavities. Accordingly a rapid phase change with a ringing following the gap is clearly found. As mentioned in the previous section, the rapid phase change with ringing is attributed to the parasitic modes of ARES. Figure 16 shows a plot of Fig. 15 zoomed in around the empty gap. A rapid phase change at the leading part of the train is 6.5 degrees (pk-pk). In Fig. 15, except the leading part, a phase modulation of about 2

ISBN 978-3-95450-187-8

degrees due to the bunch gap transient is found along the train, which agrees with the simple analytical estimation.

From the simulation results shown in Figs. 15 and 16, the rapid phase change in the leading part of the bunch train due to the bunch gap will be significantly larger in SuperKEKB. Figure 17 shows the phase difference between LER and HER ($\Delta\phi_{HER}$-$\Delta\phi_{LER}$), obtained from Fig. 15. In the figure, a plot zoomed in around the gap is presented and the solid red line indicates the relative phase. As seen in the figure, the maximum phase difference will be 5.5 degrees at the leading bunches. Besides the leading bunches, the phase difference along the train is not so large. The relative phase shift at the interaction point (IP) will be $\pm(\Delta\phi_{HER}$-$\Delta\phi_{LER})/4$ = ±1.4 degrees, excluding the leading part of the bunch train. The 1.4-degree phase shift corresponds to a longitudinal displacement of 0.44 σ_z at the IP, where the bunch length (σ_z) is 5 mm (rms).

Table 3: SuperKEKB parameters for the estimation of the bunch gap transient effect

Parameter	LER	HER
Beam energy [GeV]	4	7
Beam current [A]	3.6	2.6
Bunch gap length [%]	2	2
Beam power [MW]	8	8.3
Bunch length [mm] (rms)	6	5
RF frequency [MHz]	508.887	
Harmonic number	5120	
Revolution frequency [kHz]	99.4	
Cavity type	ARES	SCC/ARES
Number of cavities	22	8/8
Total RF voltage [MV]	10~11	15~16
Loaded Q of cavity [×10^4]	2.4	7.0/2.0
Coupling factor (β)	4.3	- /5
RF voltage/cavity [MV]	0.48	1.5/0.5
Wall loss/cavity [kW]	140	- /150
Beam power/cavity [kW]	460	400/600
Cavity detuning [kHz]	-28	-18/-44
(A-Cav detuning of ARES)	(-280)	(-180)
Number of klystrons	18	8/8
Klystron power [kW]	~600	~450/~800

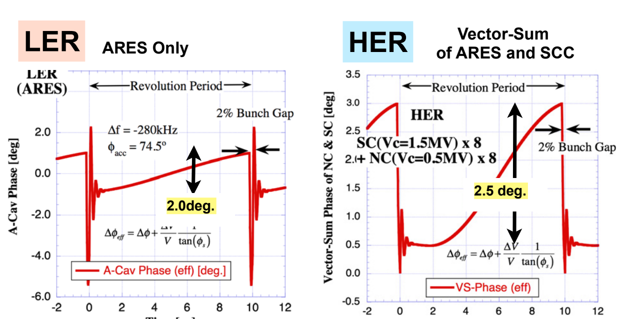

Figure 15: The simulation results of the phase modulation caused by the bunch gap transient in LER (left side) and HER (right side) for SuperKEKB design current.

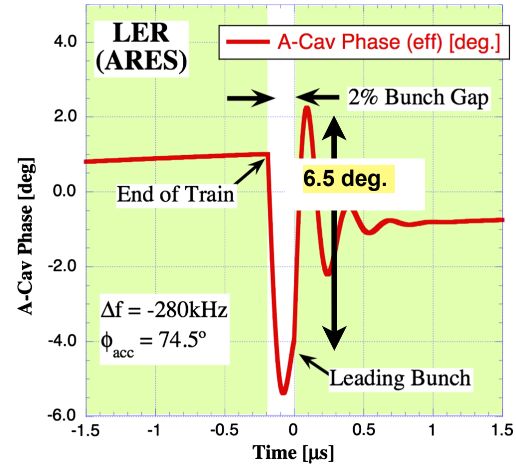

Figure 16: A plot of the simulated phase modulation shown in Fig. 15, enlarged to show the empty gap region.

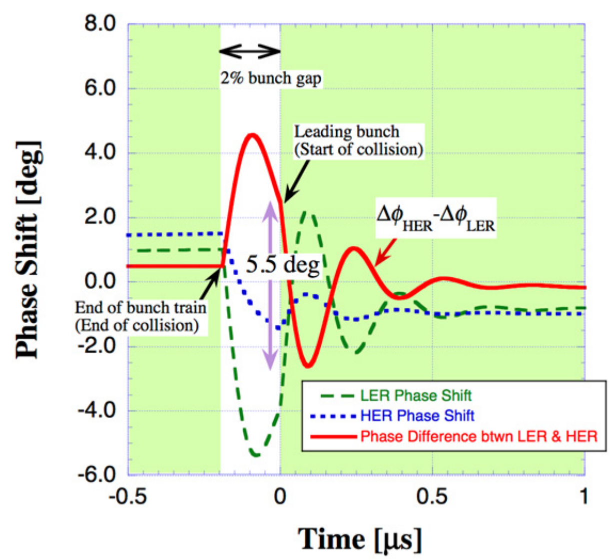

Figure 17: Plot of the phase difference between LER and HER (red solid line = $\Delta\phi_{HER}$-$\Delta\phi_{LER}$), which is zoomed in around the gap.

MITIGATION OF THE RELATIVE PHASE DIFFERENC FOR superKEKB

In the KEKB operation, no degradation was observed of the luminosity due to the bunch gap transient. However, in the SuperKEKB operation, the beam phase difference due to the gap transient will be much larger than that of KEKB, as presented in the previous section. Because the crossing angle between the two beams at the collision point is larger in SuperKEKB and the vertical beta function (β_y*) is much smaller than for KEKB, the effect of the large phase difference on the colliding beams might be a crucial issue to achieve high luminosity.

We propose measures to mitigate the phase difference between the colliding beams as a cure if the beam-beam interaction effect turns out to be critical [20]. It should be

ISBN 978-3-95450-187-8

noticed that feed-forward control cannot be available in our RF system for the measures to reduce the phase modulation due to the gap transient, because the klystron performance (bandwidth, output power) is not enough to cancel the rapid phase modulation. Consequently, we investigated the method of changing the bunch fill pattern and gap delay for the mitigation of the phase difference between two rings. The mitigation method is that LER bunch train is to be filled up in two steps with making a delay of the HER gap timing with respect to the LER gap at the cost of a reduced number of colliding bunches as shown in Fig. 18. For the simplest case, the first step increase (b_s) is set to half of the nominal bunch current. Then, the HER gap delay (d_g) and the time interval of the first step (w_s) are parameters to be optimized.

Simulation result for the best case of the fill pattern is shown in Fig. 19an 20. In this case, the length of the initial step (w_s) is 140 ns and the delay of the HER gap (d_g) is 160 ns. In this optimization, d_g was decided to synchronize the LER phase ringing with the HER phase change, and w_s was optimized to mostly cancel the phase change each other after the second step. As the result, the phase difference between two rings is significantly reduced to 0.4 degrees at the leading part of the collision as shown in Fig. 20, while the entire phase difference along the train is kept sufficiently small as shown in Fig. 19.

The effects of the proposed mitigation method are summarized in Table 4. From this summary, it is found that the fill pattern change with a HER gap delay gives a more effective mitigation compared with only the gap delay cases. However, it should be noted that this result here is an example of certain conditions. In reality, the optimization depends on strongly operation conditions. The operation conditions will be optimized for the luminosity in future SuperKEKB. The best optimization for the fill pattern and gap delay will be investigated based on the best operation conditions.

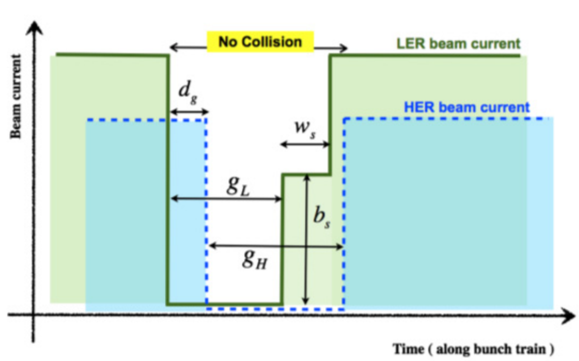

Figure 18: Illustration of a bunch fill pattern for effective mitigation. The bunch current at the leading part of the LER train is increased in two steps with a time interval w_s and the bunch current at the first step by b_s. The gap lengths are g_L and g_H for LER and HER, respectively, and the HER gap is delayed by d_g.

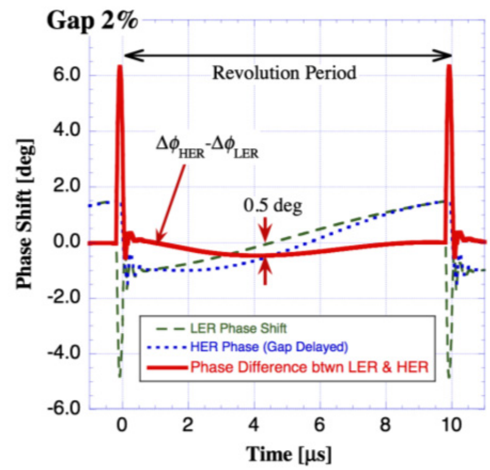

Figure 19: Simulation result of phase difference for the best case of the fill pattern shown in Fig. 18. The gap length of both rings is 2% (200 ns), the current height at the initial step of the LER leading part (b_s) is half of the nominal current, the length of the initial step (w_s) is 140 ns and the delay of the HER gap (d_g) is 160 ns.

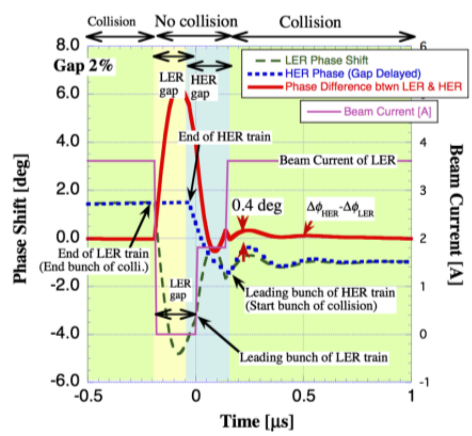

Figure 20: Zoomed plot of Fig. 19, which shows the vicinity of the gap region.

SUMMARY

Phase-1 Beam Commissioning of SuperKEKB was successfully accomplished. Desired Beam current in the two rings was achieved and sufficient vacuum scrubbing was progressed.

Newly developed digital LLRF control systems are applied to 9 stations at OHO section, and successfully worked in Phase-1.

The μ=-1 mode damper is applied to HER, and the coupled bunch instability due to detuned cavities is suppressed successfully. The μ=-2 and -3 mode damper system is now under development for Phase-2

Phase modulation due to bunch gap transient effect will be too large at the leading part of the bunch train for design beam current. Simulation study proposes the measures to mitigate the phase difference: the relative phase change at the IP can be reduced by optimization of the gap delay and bunch fill pattern of LER.

ISBN 978-3-95450-187-8

Table 4: Effects of the proposed mitigation methods on reducing the phase difference between colliding beams.

Method	Bunch Gap	HER delay	Relative Phase Difference $\|\Delta\varphi_{HER} - \Delta\varphi_{LER}\|$ Leading Part	[deg.]	The rest of train	Longitudinal displacement @IP (σ_z = 5 mm)	Rate of num. of colliding bunches
HER Gap Delay Only	2%	no delay	5.5	[deg.]	0.9	0.44 σ_z	-
	2%	200 ns	2.4		0.9	0.19 σ_z	-2%
	3%	300 ns	< 0.2		1.6	0.13 σ_z	-4%
LER 2-step fill up + HER Gap Delay	2%	160 ns	0.4	[deg.]	0.5	0.07 σ_z	-1.6%

REFERENCES

[1] T. Abe, et al., "KEKB Accelerator," Prog. Theor. Exp. Phys. 2013, Special Section (2013)

[2] P. B. Wilson, "Beam Loading in High Energy Storage Rings," PEP-Note 37, SPEAR-163 (1973)

[3] K. Akai, et al., "RF systems for the KEK B-Factory," Nucl. Instrum. Meth. A 499, 45–65 (2003)

[4] T. Abe, et al., "Performance and operation results of the RF systems at the KEK B-Factory", Prog. Theor. Exp. Phys. 2013, 03A006 (2013)

[5] Y. Yamazaki and T. Kageyama, "A Three-Cavity System which Suppresses the Coupled-Bunch Instability Associated with the Accelerating Mode," Part. Accel., 44, 107 (1994)

[6] T. Kageyama, et al., "The ARES cavity for KEKB," Conf. Proc. of APAC98, pp. 773-775 (1998)

[7] T. Furuya, et al., "A Prototype Module of a Superconducting Damped Cavity for KEKB," Conf. Proc. of EPAC96, pp. 2121-2123 (1996)

[8] S. Mitsunobu, et al., "Superconducting cavities for KEK B factory," Adv. Cryog. Eng. 45A, 861-870 (2000)

[9] T. Kageyama, at al., "ARES Cavity System for SuperKEKB," Proc. of the 8th annual meeting of Particle Accelerator Society of Japan, pp. 1245-1249 (2011)

[10] K. Akai, "RF Issues for High Intensity Factories," Conf. Proc. of EPAC96, pp. 205-209 (1996)

[11] Y. Ohnishi, et al., "Accelerator design at SuperKEKB," Prog. Theor. Exp. Phys. 2013, 03A011 (2013)

[12] T. Abe, et al., "Belle II Technical Design Report," KEK Report 2010-1 (2010)

[13] K. Akai, et al., "RF system for SuperKEKB," Proc. of the 7th annual meeting of Particle Accelerator Society of Japan, pp. 1232-1236 (2010)

[14] T. Kobayashi, et al., "Development and Construction Status of New LLRF Control System for SuperKEKB," Conf. Proc. of IPAC2014, pp. 2444-2446 (2014)

[15] M. Ryoshi et al., "LLRF Board in Micro-TCA Platform," Proc. of the 7th Annual Meeting of Particle Acc. Society of Japan, p. 668 (2010).

[16] J. Odagiri et al., "Fully Embedded EPICS-Based Control of Low Level RF System for SuperKEKB," Proc. of IPAC'10, p. 2686 (2010).

[17] T. Kobayashi, et al., "RF Reference Distribution System for SuperKEKB," Proc. of the 10th Annual Meeting of Particle Accelerator Society of Japan, pp. 1159-1163 (2013)

[18] K. Hirosawa, et al., "Development of a Coupled Bunch Instability Damper Caused by the Acceleration Mode for SuperKEKB," Proc. of the 13th Annual Meeting of Particle Accelerator Society of Japan, TUP012 (2016)

[19] D. Boussard, "RF Power Requirements for High Intensity Proton Collider," Conf. Proc. of PAC91, pp. 2447-2449 (1991)

[20] T. Kobayashi and K. Akai, "Advanced simulation study on bunch gap transient effect" Phys. Rev. Accel. Beams 19, 062001 (2016)